Supplementary Information (SI) for Physical Chemistry Chemical Physics.

Decomposition of organometallic precursor tricarbonyl(trimethylenemethane)ruthenium $Ru(C_4H_6)(CO)_3^{+/0}$ in the gas phase investigated by thermal desorption spectrometry

Ken Miyajima*[,a], Toshiaki Nagata[b], Fumitaka Mafuné[b], Tomohiro Tsugawa[c], and Ryosuke Harada[c]

[a] *KOMEX, School of Arts and Sciences, The University of Tokyo, Komaba, Meguro, Tokyo 153-8902, Japan,*

[b] *Department of Basic Science, School of Arts and Sciences, The University of Tokyo, Komaba, Meguro, Tokyo 153-8902, Japan,*

[c] *Chemical Materials Development Department, Global Marketing / R&D Supervisory Department, TANAKA PRECIOUS METAL TECHNOLOGIES Co., Ltd., 22, Wadai, Tsukuba, Ibaraki 300-4247, Japan*

Contents

Fig. S1 Schematic of the cluster source equipped with a temperature-variable extension tube.

Fig. S2 Mass spectra of the species produced by thermal decomposition of $Ru(C_4H_6)(CO)_3^+$ in 0.17% O_2 seeded helium carrier gas at 303 and 1020 K.

Fig. S3 Mass spectra of the positively charged species produced by the laser ablation of Ru rod in $Ru(C_4H_6)(CO)_3$ vapor seeded 0% and 0.17% O_2 seeded helium carrier gas at 303 K.

Fig. S4 Structural changes and differences in the formation energies of CO and H_2 desorption processes.

Fig. S5 (a) Estimated activation energies for the thermal decomposition reactions of $Ru(C_4H_6)(CO)_3^+$ obtained by curve fitting and (b) model of the reaction network path.

Fig. S6 Structures of $Ru(C_4H_6)(CO)_{0–3}^+$ in the quartet spin state.

Fig. S7 Structures of $RuC_4H_4^+$ in the quartet spin state.

Fig. S8 Structures of $Ru(C_4H_6)(CO)_{0–3}$ in the triplet spin state.

Fig. S9 Structures of RuC_4H_4 in the second most stable spin state.

Table S1 Atomic coordinates of DFT-calculated structures and natural charges and spins of atoms obtained by NBO analysis.

Table S2 The HOMO energies and the ionization energies.

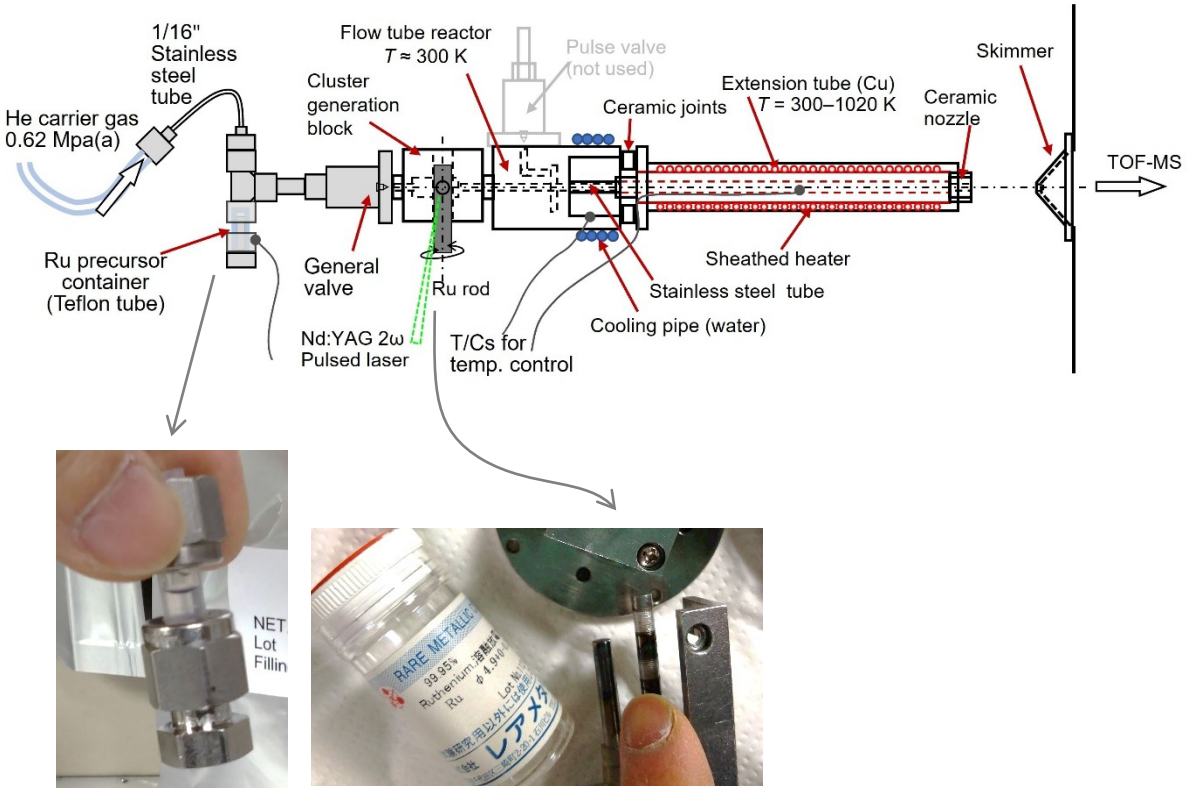

Fig. S1 Schematic of the cluster source equipped with a temperature-variable extension tube. A liquid of $Ru(C_4H_6)(CO)_3$ was loaded into a short 1/4-inch Teflon tube connected via an inch stainless-steel T-joint to the helium carrier gas line upstream of the general valve. The end of the Teflon tube was sealed with a stainless-steel end cap (left photo), allowing the liquid to vaporize and mix with helium flow. The right photograph shows a Ru metal rod with helical grooves engraved by laser ablation after the experiment.

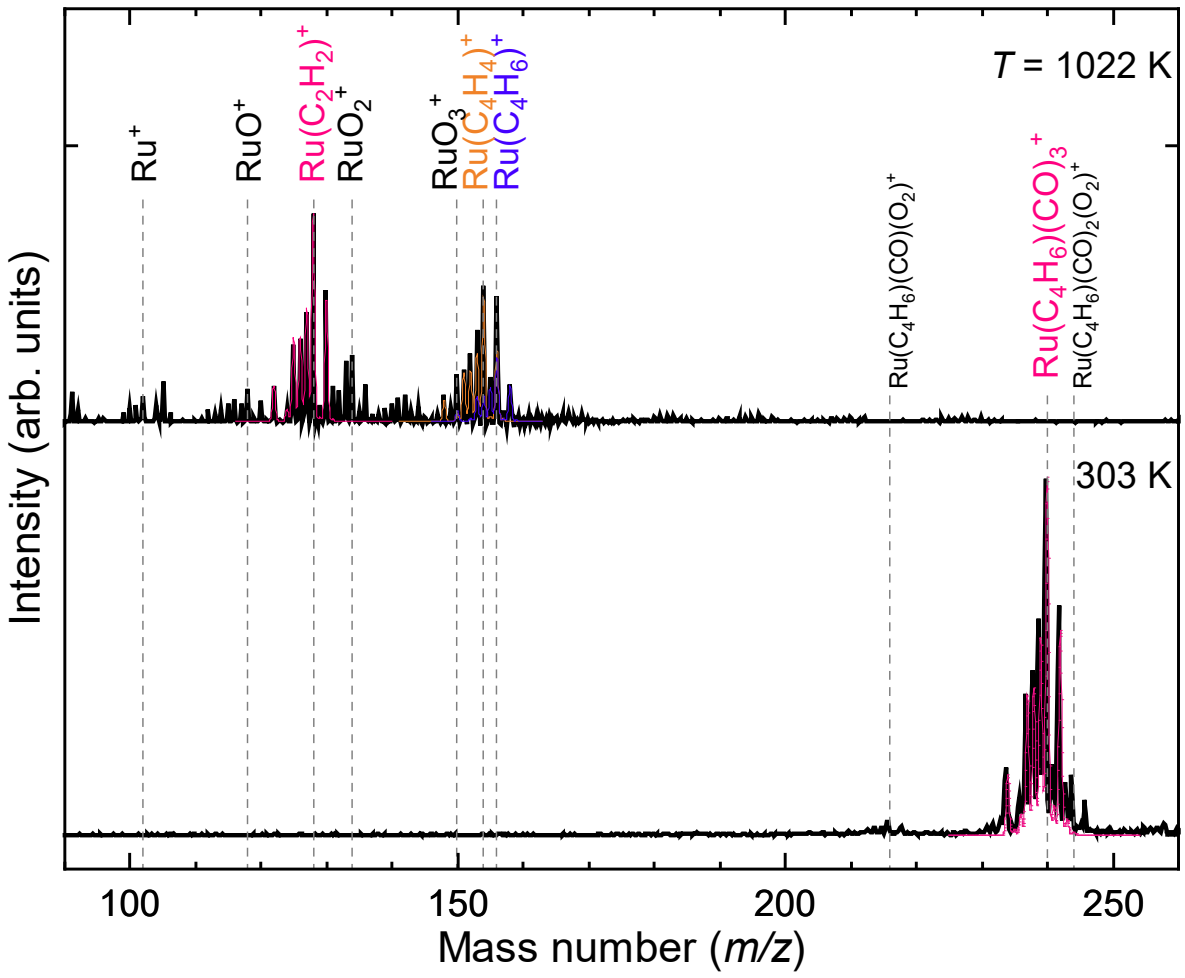

Fig. S2 Mass spectra of the species produced by the thermal decomposition of $Ru(C_4H_6)(CO)_3^+$ in 0.17% O_2 seeded helium carrier gas at 303 and 1020 K. The solid black line represents the mass spectrum. Pink, orange, and purple represent the distributions of the peaks corresponding to each composition caused by the isotopic distribution of Ru.

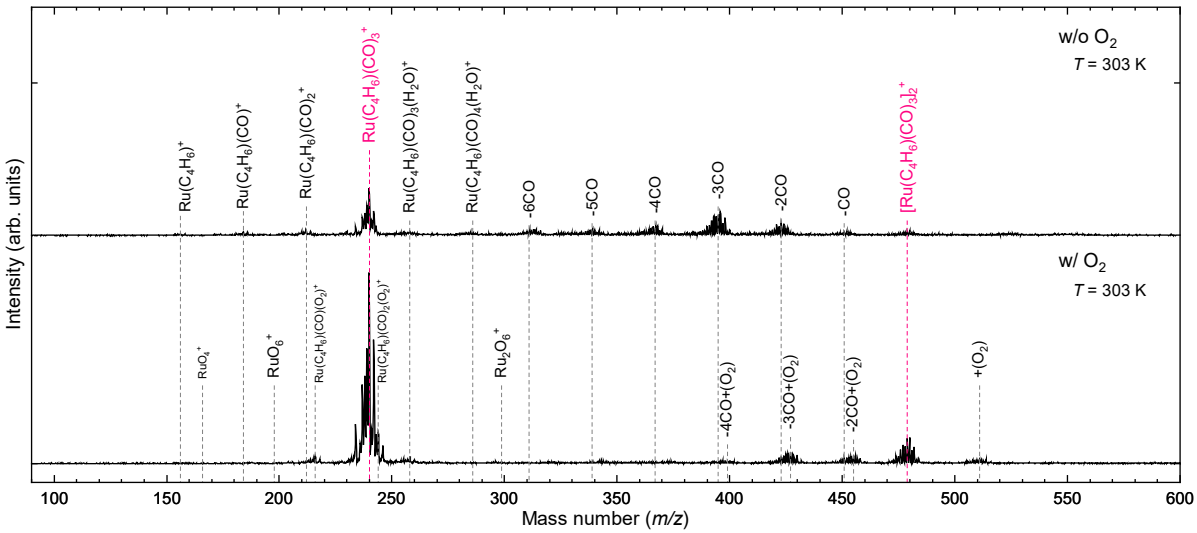

Fig. S3 Mass spectra of the positively charged species produced by the laser ablation of the Ru rod in $Ru(C_4H_6)(CO)_3$ vapor seeded at 0% and 0.17% O_2 seeded helium carrier gas at 303 K. The monomers and dimers of $Ru(C_4H_6)(CO)_3$ are labeled pink.

(a) Cations

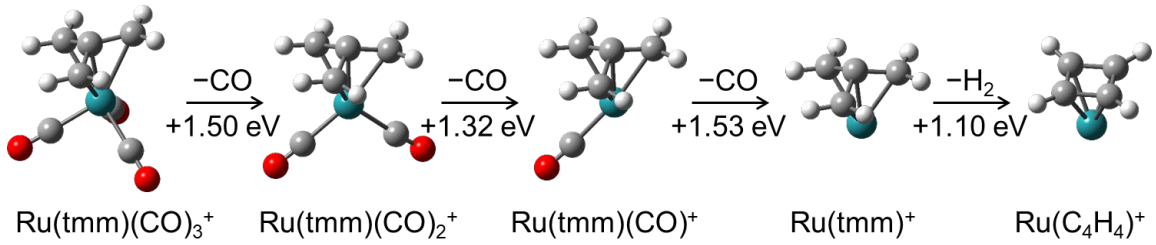

(b) Neutrals

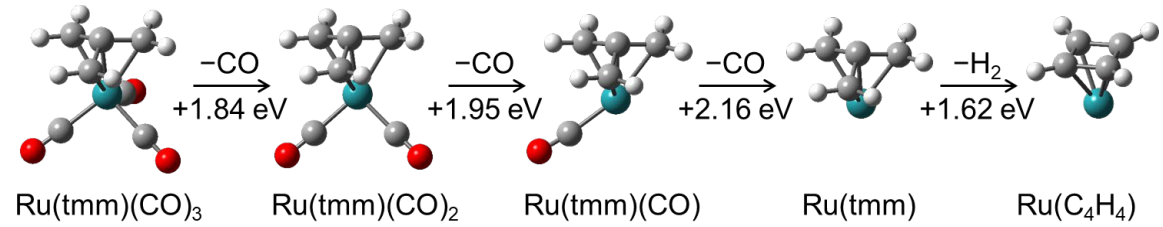

Fig. S4 Structural changes and differences in the formation energies of CO and H_2 desorption processes. (a) Cations. Calculations were performed for the doublet and quartet, and the doublet was found to be stable in all cases. (b) Neutrals. Calculations were performed for singlet and triplet, and the singlet was stable in all cases. Here, tmm denotes trimethylenemethane, C_4H_6.

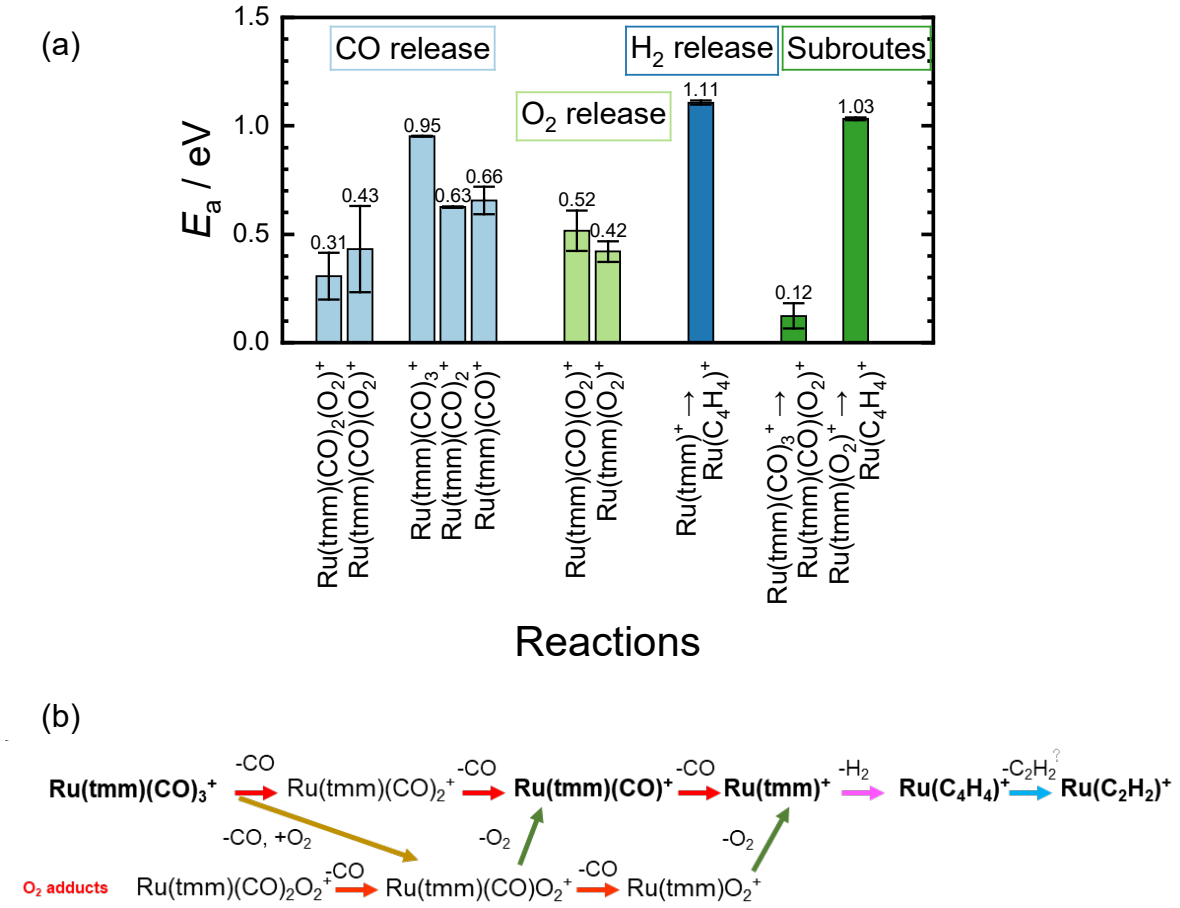

Fig. S5 (a) Estimated activation energies for the thermal decomposition reactions of $Ru(C_4H_6)(CO)_3^+$ obtained by curve fitting, and (b) model of the reaction network path.

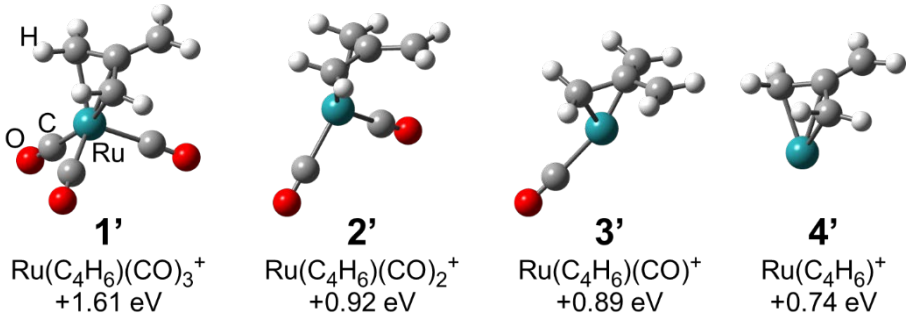

Fig. S6 Structures of $Ru(C_4H_6)(CO)_{0–3}^+$ in the quartet spin state and the relative energies to the corresponding stable structures in the doublet spin state. The doublet structures are given in Fig. 4 of the main text.

For the cations, the doublet spin state is the most stable, and the quartet spin state is the second most stable. The quartet $Ru(C_4H_6)(CO)_{0–3}^+$ structures are a little different from the doublet structures: The distance between one of the C atoms of the C_4H_6 ligand and the Ru atom is elongated compared to the corresponding doublet structures. The quartet energies are ca. 0.7–1.6 eV higher than the doublet energies.

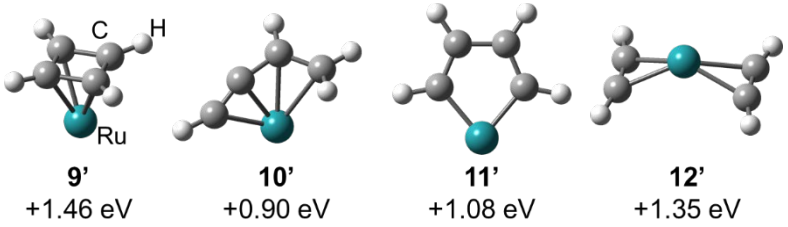

Fig. S7 Structures of $RuC_4H_4^+$ in the quartet spin state and the relative energies to the most stable isomer, **9** in the doublet spin state. The doublet structures and their relative energies are given in Fig. 6 of the main text.

The quartet structures of $RuC_4H_4^+$ resemble the corresponding doublet structures. The quartet structure 9' has an energy 1.46 eV higher than the doublet structure 9. The other isomers show relatively small energy differences (ca. 0.2–0.3 eV) from the corresponding doublet isomers.

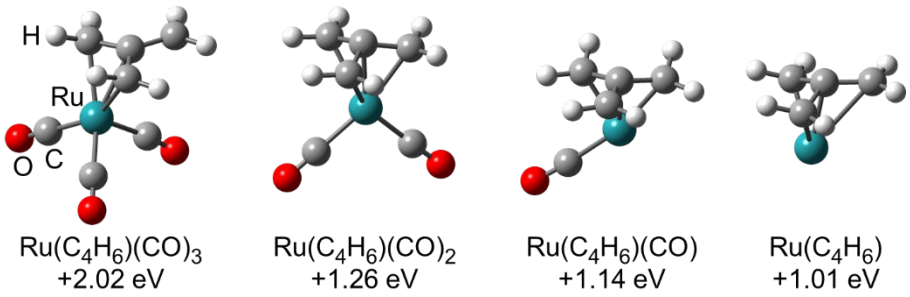

Fig. S8 Structures of $Ru(C_4H_6)(CO)_{0–3}$ in the triplet spin state and the relative energies to the corresponding stable structures in the singlet spin state. The singlet structures are given in Fig. S4 of Supplementary Information.

For the neutral $Ru(C_4H_6)(CO)_{0–3}$, the singlet spin state is the most stable and the triplet state is the second most stable. The triplet structures show asymmetric coordination of the C_4H_6 ligand unlike the singlet structures. The energies are ca. 1.0–2.0 eV higher for the quartet than those for the singlet.

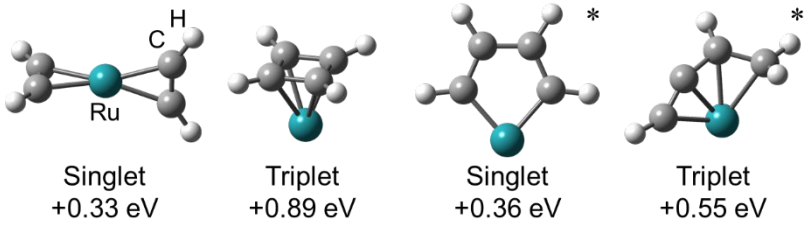

Fig. S9 Structures of RuC_4H_4 in the second most stable spin state and the relative energies to the most stable isomer, the triplet $Ru(C_2H_2)_2$. Structures of the most stable spin state are shown in Fig. 7 of the main text. The structures are arranged in the same order as in Fig.7. Note that the two structures marked with * show imaginary vibrations of the ligand out-of-plane distortion mode, which could not be removed during our geometric optimization processes.

For $RuC_4H_4^+$, the most stable spin state is singlet or triplet, dependent on the isomer, as shown in Fig. 7. The second most stable spin state shows similar structures.

Table S1 Atomic coordinates of DFT-calculated structures and natural charges and spins of atoms obtained by NBO analysis. These numbers correspond to the structures shown in Fig. 4, 6, 7 and S4, respectively.

1 $Ru(C_4H_6)(CO)_3^+$

	x	*y*	*z*	charge	spin
Ru	-0.015745	0.000014	-0.129479	-0.98673	0.27659
C	-0.773724	0.000027	1.585694	0.88143	0.03089
C	-1.168076	-1.494214	-0.711674	0.80626	0.00464
C	-1.168351	1.493967	-0.711775	0.80627	0.00465
O	-1.808675	2.367994	-1.009511	-0.34783	0.01841
O	-1.202018	0.000008	2.628238	-0.36011	-0.00190
O	-1.808237	-2.368377	-1.009358	-0.34784	0.01840
C	2.092793	0.000147	0.052558	-0.07896	-0.06994
C	2.198806	-0.000070	-1.372714	-0.13720	0.59868
C	1.699633	-1.225510	0.656245	-0.34046	0.08184
C	1.699424	1.225928	0.655878	-0.34052	0.08176
H	2.314488	-0.928656	-1.916979	0.23073	-0.01651
H	2.314294	0.928376	-1.917265	0.23073	-0.01651
H	1.892175	-2.150995	0.131206	0.24558	-0.00259
H	1.674264	-1.301144	1.734852	0.24653	-0.00291
H	1.891874	2.151288	0.130585	0.24558	-0.00259
H	1.674076	1.301872	1.734463	0.24654	-0.00291

2 $Ru(C_4H_6)(CO)_2^+$

	x	*y*	*z*	charge	spin
Ru	-0.026719	0.055327	0.000000	-0.23314	1.04766
C	1.136329	1.655116	0.000000	0.70447	-0.00663
C	-1.894847	0.964775	0.000000	0.70667	0.03739
O	1.830899	2.539424	0.000000	-0.35030	-0.00234
O	-2.924408	1.401217	0.000000	-0.31844	-0.00242
C	0.531638	-1.937907	0.000000	-0.03272	0.01195
C	-0.877072	-2.018397	0.000000	-0.39976	-0.00242
C	1.136329	-1.347846	1.158127	-0.28344	-0.05257
C	1.136329	-1.347846	-1.158127	-0.28344	-0.05257
H	-1.392673	-2.273749	0.916708	0.24672	0.00026
H	-1.392673	-2.273749	-0.916708	0.24672	0.00026
H	0.644912	-1.434069	2.123336	0.25000	0.00751
H	2.203490	-1.175635	1.182213	0.24833	0.00321
H	0.644912	-1.434069	-2.123336	0.25000	0.00751
H	2.203490	-1.175635	-1.182213	0.24833	0.00321

3 $Ru(C_4H_6)(CO)^+$

	x	*y*	*z*	charge	spin
Ru	0.086151	-0.447737	0.000001	0.38324	1.14796
C	2.017194	0.018048	-0.000003	0.59295	-0.00695
O	3.087968	0.357913	0.000001	-0.33845	-0.01151
C	-1.609521	0.708560	-0.000000	-0.04299	0.01737
C	-2.181692	-0.566186	-0.000001	-0.39306	-0.06043
C	-0.825718	1.050768	-1.164555	-0.34411	-0.05693
C	-0.825720	1.050769	1.164554	-0.34411	-0.05693
H	-2.569183	-0.985603	-0.919740	0.24457	0.00157
H	-2.569186	-0.985604	0.919735	0.24457	0.00157
H	-1.094493	0.619934	-2.125654	0.25039	0.00930
H	-0.307133	1.998362	-1.208317	0.24830	0.00284
H	-1.094495	0.619935	2.125654	0.25039	0.00930
H	-0.307135	1.998362	1.208317	0.24830	0.00284

4 $Ru(C_4H_6)^+$

	x	*y*	*z*	charge	spin
Ru	0.687965	0.000375	-0.007948	0.74025	1.18651
C	-1.313376	-0.000673	0.014127	-0.03582	0.01232
C	-0.903676	1.153063	0.762194	-0.39865	-0.07687
C	-0.903994	-1.227503	0.635358	-0.39854	-0.07686
C	-0.944907	0.072812	-1.363610	-0.38273	-0.07313
H	-0.956204	1.144377	1.844175	0.24633	0.00415
H	-0.957525	2.132043	0.300124	0.24946	0.00803
H	-0.956450	-1.333804	1.712154	0.24629	0.00411
H	-0.958000	-2.151843	0.071908	0.24945	0.00802
H	-1.023224	1.019105	-1.884609	0.24196	0.00185
H	-1.023328	-0.812579	-1.982456	0.24199	0.00187

5 $Ru(C_4H_4)(CO)_3(H_2)^+$

	x	*y*	*z*	charge	spin
Ru	0.007848	0.003805	-0.096701	-1.05131	0.56257
C	1.933255	0.766192	-0.768067	-0.12720	0.09424
C	1.931273	-0.707451	-0.822194	-0.13120	0.08590
C	1.937665	-0.759008	0.597981	-0.12426	0.06108
C	1.937603	0.714860	0.652022	-0.12791	0.05579
H	2.043073	1.554473	-1.495202	0.28227	-0.00256
H	2.042389	-1.440928	-1.604332	0.28236	-0.00234
H	2.079749	1.444902	1.431629	0.28103	-0.00213
H	2.079590	-1.544243	1.322107	0.28090	-0.00228
H	-0.040177	-0.195502	-3.331082	0.00309	0.00465
H	-0.086927	0.548172	-3.331650	0.01127	0.00599
C	-1.188544	-1.486889	-0.629289	0.81093	0.01337
O	-1.837782	-2.355450	-0.923194	-0.34704	0.03388
C	-0.618469	-0.080714	1.740498	0.84852	0.04758
O	-0.941684	-0.130788	2.816589	-0.35577	-0.00261
C	-1.188284	1.537990	-0.486917	0.81148	0.01342
O	-1.836782	2.430718	-0.698497	-0.34717	0.03343

6 $Ru(C_4H_4)(CO)_2(H_2)^+$

	x	*y*	*z*	charge	spin
Ru	0.010560	-0.093868	-0.402352	-0.85448	0.67918
C	-2.135351	-0.461657	-0.393784	-0.14210	0.01400
C	-1.882301	0.771858	0.272445	-0.11628	0.09159
C	-1.199823	0.051400	1.354795	-0.13838	0.00018
C	-1.482339	-1.189933	0.694327	-0.12116	0.12192
H	-2.697528	-0.744358	-1.269526	0.28301	-0.00033
H	-2.193655	1.791805	0.115956	0.28000	-0.00307
H	-1.385657	-2.228718	0.966413	0.28223	-0.00312
H	-0.859033	0.316766	2.341669	0.28103	-0.00033
H	-0.050586	0.168420	-2.211560	0.16052	0.00090
H	0.750635	0.037588	-2.084435	0.16632	0.00361
C	0.898933	1.589038	0.075982	0.82295	0.05318
O	1.370551	2.559074	0.391679	-0.35194	0.00144
C	1.622917	-1.109210	0.129726	0.79546	0.01667
O	2.509317	-1.699109	0.488820	-0.34719	0.02417

7 $Ru(C_4H_4)(CO)(H_2)^+$

	x	*y*	*z*	charge	spin
Ru	-0.083770	-0.462256	-0.139088	-0.03076	1.02150
C	1.927600	-0.140703	0.596953	-0.18735	0.01961
C	0.983240	0.897699	1.013644	-0.11110	-0.05222
C	0.914839	1.371161	-0.356960	-0.20344	0.02578
C	1.860684	0.336082	-0.741580	-0.13382	-0.04727
H	2.522540	-0.877950	1.111202	0.28036	-0.00058
H	0.659041	1.289735	1.964458	0.27623	0.00163
H	2.346856	0.059053	-1.664916	0.27595	0.00147
H	0.521120	2.255911	-0.829140	0.28101	0.00017
H	-0.889415	-1.861320	0.819214	0.10928	0.00386
H	-0.096726	-1.957216	0.976695	0.10877	0.00875
C	-1.952455	0.213973	-0.016629	0.67661	0.01835
O	-2.972624	0.670220	0.096224	-0.34173	-0.00107

8 $Ru(C_4H_4)(H_2)^+$

	x	*y*	*z*	charge	spin
Ru	0.655912	0.122890	0.000001	0.46611	1.14521
C	-1.288659	0.601866	0.712527	-0.19057	-0.03809
C	-1.033908	-0.838306	0.723498	-0.16944	-0.04359
C	-1.033893	-0.838379	-0.723428	-0.16945	-0.04359
C	-1.288641	0.601795	-0.712603	-0.19056	-0.03808
H	-1.489120	1.345268	1.468365	0.27576	0.00126
H	-1.037363	-1.610200	1.476587	0.27652	0.00170
H	-1.489088	1.345131	-1.468511	0.27576	0.00126
H	-1.037339	-1.610342	-1.476444	0.27652	0.00170
H	1.758637	-1.324581	-0.000002	0.08846	-0.00178
H	2.304739	-0.714311	-0.000017	0.06090	0.01400

9 $Ru(C_4H_4)^+$

	x	*y*	*z*	charge	spin
Ru	-0.708756	-0.000000	-0.000000	0.69784	1.19932
C	1.098683	1.023684	-0.067620	-0.19805	-0.05100
C	1.098684	-0.067620	-1.023684	-0.19805	-0.05100
C	1.098684	-1.023684	0.067620	-0.19805	-0.05100
C	1.098683	0.067620	1.023684	-0.19805	-0.05100
H	1.204219	2.094590	-0.138953	0.27359	0.00117
H	1.204216	-0.138953	-2.094590	0.27359	0.00117
H	1.204216	0.138953	2.094590	0.27359	0.00117
H	1.204218	-2.094590	0.138953	0.27359	0.00117

10 $Ru(C_4H_4)^+$

	x	*y*	*z*	charge	spin
Ru	-0.335079	-0.531847	-0.059510	0.78759	1.07075
C	-1.092594	1.403975	0.289698	-0.24474	-0.03746
C	0.087786	1.513897	-0.114129	0.06132	0.00874
C	1.243650	0.806784	-0.459989	-0.24240	-0.02001
C	1.612650	-0.148119	0.536496	-0.44189	-0.02804
H	-2.004278	1.816549	0.679047	0.29087	-0.00051
H	1.569457	0.122899	1.587275	0.25428	0.00314
H	2.359534	-0.890009	0.272455	0.25403	0.00077
H	1.709826	0.892611	-1.432808	0.28096	0.00264

11 $Ru(C_4H_4)^+$

	x	*y*	*z*	charge	spin
Ru	-0.000096	-0.826293	-0.000000	0.67915	1.40737
C	0.000146	0.580658	1.218797	-0.14857	-0.18478
C	0.000146	1.909960	0.682323	-0.15958	-0.03179
C	0.000146	1.909960	-0.682323	-0.15958	-0.03179
C	0.000146	0.580658	-1.218797	-0.14857	-0.18478
H	0.000223	0.433319	2.301555	0.21732	0.01104
H	0.000145	2.801415	1.296193	0.25125	0.00184
H	0.000223	0.433319	-2.301555	0.21732	0.01104
H	0.000145	2.801415	-1.296193	0.25125	0.00184

12 $Ru(C_2H_2)_2^+$

	x	*y*	*z*	charge	spin
Ru	-0.000001	0.384311	0.200382	0.56161	0.87517
C	-1.683023	-0.077835	-0.670474	-0.21167	-0.00691
C	-1.337660	-1.046723	0.095330	-0.12408	0.07632
C	1.337669	-1.046715	0.095335	-0.12408	0.07632
C	1.683021	-0.077830	-0.670478	-0.21167	-0.00691
H	-2.348671	0.351826	-1.401994	0.28265	-0.00242
H	-1.452100	-2.059371	0.444462	0.27230	-0.00458
H	2.348652	0.351818	-1.402022	0.28265	-0.00242
H	1.452121	-2.059355	0.444486	0.27230	-0.00458

$Ru(C_4H_6)(CO)_3$

	x	*y*	*z*	charge	spin
Ru	-0.008725	-0.000024	-0.000153	-1.41729	0.00000
C	-0.983604	1.550062	0.582736	0.86216	0.00000
C	-0.983941	-1.278694	1.051699	0.86220	0.00000
C	-0.986238	-0.270477	-1.632186	0.86219	0.00000
O	-1.527495	-0.433779	-2.617354	-0.44818	0.00000
O	-1.522801	2.485699	0.934889	-0.44817	0.00000
O	-1.523279	-2.050733	1.686714	-0.44818	0.00000
C	2.065053	-0.000467	-0.001490	0.00555	0.00000
C	1.729487	-1.300597	-0.489300	-0.38721	0.00000
C	1.731746	0.226967	1.368759	-0.38713	0.00000
C	1.730391	1.072295	-0.883352	-0.38716	0.00000
H	1.858468	-2.149844	0.168569	0.22186	0.00000
H	1.857449	-1.507226	-1.543635	0.22187	0.00000
H	1.860724	-0.582806	2.074637	0.22188	0.00000
H	1.860779	1.221389	1.775125	0.22186	0.00000
H	1.858216	0.926937	-1.947870	0.22188	0.00000
H	1.859510	2.088584	-0.535273	0.22187	0.00000

$Ru(C_4H_6)(CO)_2$

	x	*y*	*z*	charge	spin
Ru	0.034797	0.000000	-0.325984	-0.60591	0.00000
C	1.277370	-1.408218	-0.032819	0.73662	0.00000
C	1.277369	1.408218	-0.032813	0.73663	0.00000
O	1.984478	-2.264179	0.225766	-0.45610	0.00000
O	1.984479	2.264179	0.225764	-0.45610	0.00000
C	-1.864215	0.000001	0.458957	-0.01713	0.00000
C	-1.840676	1.215176	-0.275095	-0.45737	0.00000
C	-0.918046	-0.000004	1.558030	-0.33619	0.00000
C	-1.840678	-1.215172	-0.275100	-0.45737	0.00000
H	-1.771368	2.150102	0.263748	0.22108	0.00000
H	-2.350050	1.261942	-1.230962	0.21865	0.00000
H	-0.793310	0.911141	2.129259	0.21673	0.00000
H	-0.793314	-0.911153	2.129253	0.21673	0.00000
H	-2.350053	-1.261933	-1.230967	0.21865	0.00000
H	-1.771373	-2.150100	0.263741	0.22108	0.00000

$Ru(C_4H_6)(CO)$

	x	*y*	*z*	charge	spin
Ru	0.061518	-0.518228	0.000000	-0.01699	0.00000
C	1.865307	-0.015466	0.000003	0.59954	0.00000
O	2.918207	0.437512	-0.000001	-0.47652	0.00000
C	-1.446011	0.826949	-0.000001	-0.03225	0.00000
C	-2.199850	-0.363243	0.000000	-0.52116	0.00000
C	-0.653502	1.052896	-1.188508	-0.41504	0.00000
C	-0.653503	1.052900	1.188505	-0.41504	0.00000
H	-2.670556	-0.692825	-0.917823	0.21457	0.00000
H	-2.670557	-0.692822	0.917824	0.21457	0.00000
H	-1.062038	0.744615	-2.144891	0.21060	0.00000
H	-0.030959	1.937071	-1.232257	0.21356	0.00000
H	-1.062041	0.744623	2.144890	0.21060	0.00000
H	-0.030960	1.937075	1.232253	0.21356	0.00000

$Ru(C_4H_6)$

	x	*y*	*z*	charge	spin
Ru	0.673627	0.000164	-0.000014	0.29978	0.00000
C	-1.284980	-0.000317	0.000025	-0.04561	0.00000
C	-0.879901	-1.168486	0.747325	-0.49177	0.00000
C	-0.880403	-0.063281	-1.385368	-0.49178	0.00000
C	-0.880905	1.231142	0.638097	-0.49175	0.00000
H	-1.013019	-2.143562	0.290653	0.20351	0.00000
H	-1.013127	-1.162734	1.824016	0.20351	0.00000
H	-1.013580	-0.998669	-1.918618	0.20352	0.00000
H	-1.014022	0.819693	-2.001442	0.20353	0.00000
H	-1.014202	1.323146	1.710856	0.20353	0.00000
H	-1.014514	2.160580	0.094683	0.20353	0.00000

$Ru(C_2H_2)_2$

	x	*y*	*z*	charge	spin
Ru	0.000000	0.000025	0.000041	0.46845	2.03291
C	-1.914168	-0.446091	-0.458541	-0.34911	-0.00950
C	-1.914275	0.446000	0.458409	-0.34914	-0.00948
C	1.914209	0.458448	-0.446100	-0.34912	-0.00950
C	1.914234	-0.458505	0.445989	-0.34912	-0.00949
H	-2.509936	-1.070428	-1.100235	0.23201	0.00127
H	-2.510212	1.070261	1.100018	0.23201	0.00127
H	2.510107	-1.100155	1.070270	0.23201	0.00127
H	2.510041	1.100115	-1.070402	0.23201	0.00127

$Ru(C_4H_4)$, cyclobutadiene

	x	*y*	*z*	charge	spin
Ru	0.699507	-0.000000	0.000000	0.18239	0.00000
C	-1.079630	-0.393582	0.951556	-0.26686	0.00000
C	-1.079616	-0.951559	-0.393584	-0.26686	0.00000
C	-1.079618	0.393583	-0.951556	-0.26686	0.00000
C	-1.079621	0.951558	0.393583	-0.26686	0.00000
H	-1.216812	-0.802914	1.939344	0.22127	0.00000
H	-1.216873	-1.939338	-0.802912	0.22127	0.00000
H	-1.216859	1.939342	0.802905	0.22127	0.00000
H	-1.216839	0.802912	-1.939340	0.22127	0.00000

$Ru(C_4H_4)$, 1,3-butadiene-1,4-diyl

	x	*y*	*z*	charge	spin
Ru	-0.835987	0.000000	0.000004	0.47198	1.81694
C	0.637243	1.278445	-0.000023	-0.35898	-0.00606
C	1.876813	0.718457	0.000010	-0.25720	0.09876
C	1.876813	-0.718457	0.000010	-0.25720	0.09876
C	0.637243	-1.278445	-0.000023	-0.35898	-0.00606
H	0.512080	2.362700	-0.000040	0.17953	0.00338
H	2.795294	1.296571	0.000028	0.20066	-0.00456
H	0.512081	-2.362700	-0.000040	0.17953	0.00338
H	2.795294	-1.296571	0.000028	0.20066	-0.00456

$Ru(C_4H_4)$, 1-butene-3-yne

	x	*y*	*z*	charge	spin
Ru	-0.318036	-0.518064	-0.065055	0.27098	0.00000
C	-1.117231	1.286368	0.353143	-0.33998	0.00000
C	0.020149	1.478521	-0.203866	-0.00054	0.00000
C	1.209639	0.788865	-0.488382	-0.28800	0.00000
C	1.583222	-0.112908	0.591591	-0.52719	0.00000
H	-1.933092	1.811310	0.814176	0.23274	0.00000
H	1.636434	0.251480	1.612579	0.21469	0.00000
H	2.375808	-0.816855	0.344348	0.20655	0.00000
H	1.739764	0.903796	-1.423578	0.23075	0.00000

Table S2 The calculated HOMO energy levels. The HOMO energies and the ionization energies show a similar trend. The vertical ionization energies, calculated from the energies of the neutral and cationic states of the neutral geometries, rather than the HOMO levels, are considered appropriate for discussing the ionization capability of the 157 nm (7.87 eV) laser.

Species	Ionization energy / eV	HOMO energy / eV
$Ru(C_4H_6)(CO)_3$	9.11	−9.26
$Ru(C_4H_6)(CO)_2$	8.55	−8.85
$Ru(C_4H_6)(CO)$	7.68	−8.11
$Ru(C_4H_6)$	6.87	−7.17
$Ru(C_4H_4)$	6.15	−6.28
$Ru(C_2H_2)$ †	7.06	−7.58 (α), −6.82 (β)
RuC	7.42	−6.99

† Triplet state